Bull. Mater. Sci., Vol. 36, No. 6, November 2013, pp. 1079–1086. © Indian Academy of Sciences.

Yellow phosphors doping with Gd^{3+}, Tb^{3+} and Lu^{3+} in $MTiO_3$ (M = Mg and Sr) luminescence properties

ESRA KORKMAZ[1], NILGUN OZPOZAN KALAYCIOGLU[2,*] and V EMIR KAFADAR[3]

[1]Faculty of Science and Arts, Department of Chemistry, Bozok University, Yozgat 66900, Turkey
[2]Faculty of Science, Department of Chemistry, Erciyes University, Kayseri 38039, Turkey
[3]Department of Engineering Physics, Gaziantep University, Gaziantep 27310, Turkey

MS received 18 April 2012

Abstract. **This paper reports Gd^{3+}, Tb^{3+} and Lu^{3+} doped $MTiO_3$ (M = Mg and Sr)-based phosphors which were synthesized by the conventional solid-state reaction method, their crystal structures and luminescence properties were investigated. X-ray diffraction patterns (XRD) showed that phosphors sintered at 1000 °C for 2 h were the pure $SrTiO_3$ and $MgTiO_3$ phases. The optimization of reaction conditions was carried out by thermogravimetry and differential thermal analysis (DTA/TG) methods. Surface and elemental analyses were performed by using SEM instrument. The excitation and emission spectra were recorded by a photoluminescence spectrophotometer (PL). The thermoluminescence (TL) properties of $MgTiO_3$:RE (RE = Gd^{3+}, Tb^{3+}, Lu^{3+}) and $SrTiO_3$:RE (RE = Gd^{3+}, Tb^{3+}, Lu^{3+}) were investigated.**

Keywords. **Phosphors; Gd^{3+}; Tb^{3+} and Lu^{3+} luminescence; $MgTiO_3$; $SrTiO_3$; XRD; SEM; DTA/TG.**

1. Introduction

Recently, inorganic phosphors doped with rare-earth (RE) ions have attracted considerable interest due to their wide range of applications in solid-state lighting (Wickersheim and Lefever 1964; Blasse 1989). In the recent past, several groups have reported the photoluminescence (PL) of a variety of RE-doped phosphors showing efficient and narrow emissions in the visible region. Several phosphates, borates, aluminates, silicates, etc have been reported to be potential host matrices for phosphors (Cavalli *et al* 2003; Park *et al* 2003; Doat *et al* 2005; Naik *et al* 2009; Singh *et al* 2009). On similar lines, several titanates are also known to be promising host matrices. PL investigations of barium titanate have been extensively discussed by Moreira *et al* (2008). In addition, PL of several other titanate systems such as gadolinium, zirconium, strontium, lead, calcium and magnesium titanates are available in the literature (Park *et al* 2001; Wuled Lenggoro *et al* 2004; Freitas *et al* 2006; Lima *et al* 2006; Lina *et al* 2007). The interest in PL of these titanate based systems is due to the fact that TiO_2 group in these matrices has a relatively wide bandgap and high refractive index, which results in intense luminescence; for this reason, these titanate based compounds can find potential applications in optoelectronic devices (Jia *et al* 2006; Hu *et al* 2007). Moreover, TiO_2 structure itself possesses good mechanical strength and thus can withstand corrosive environments. The chromaticity of these titanate systems can be controlled to a large extent by suitable doping with $3d$ or $4f$ system and by controlling the various synthesis parameters (Sinha *et al* 2010).

In this study, $MgTiO_3$:RE (RE = Gd^{3+}, Tb^{3+}, Lu^{3+}) and $SrTiO_3$:RE (RE = Gd^{3+}, Tb^{3+}, Lu^{3+}) were synthesized via modified solid-state reaction at 1000 °C. The thermal behaviour, crystal structure, photoluminescence properties, thermoluminescence properties and morphological characterization were investigated.

2. Experimental

Rare-earth ions containing magnesium and strontium titanates were prepared by heating a mixture with a ratio of 1 mol of magnesium nitrate ($Mg(NO_3)_2{\cdot}6H_2O$) (AR) or strontium nitrate ($Sr(NO_3)_2$) (AR), 1 mol of tetra-*n*-butyl titanate ($Ti(OC_4H_9)_4$) (AR) and 0·01 mol of rare-earth nitrate of 99·99% purity in an air atmosphere. The weighed chemicals were ground well in an agate mortar at room temperature for 2 h. The hydrolysis of $Ti(OC_4H_9)_4$ started immediately during the grinding process, accompanied by the evaporation of *n*-butyl alcohol. As the reaction proceeded, the mixture became mushy and underwent gradual changes in colour, from colourless to white. A white sample was thus obtained. Eventually, ultrafine white powders were produced after calcination at the following temperatures; 600 °C for 2 h, 900 °C for 6 h and 1000 °C for 2 h.

DTA/TG combined systems (Perkin Elmer Diamond, USA) was used to determine the reaction conditions in the temperature range of 50–1200 °C under an inert N_2 atmosphere with a heating rate of 10 °C/min.

*Author for correspondence (nozpozan@erciyes.edu.tr)

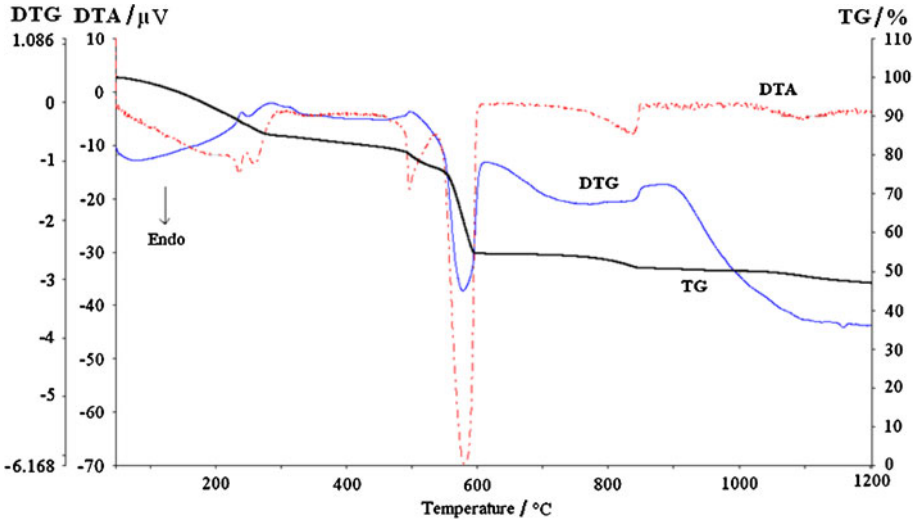

Figure 1. DTA/TG/DTG plots of stoichiometric mixture of $Sr(NO_3)_2$ and $Ti(OC_4H_9)_4$.

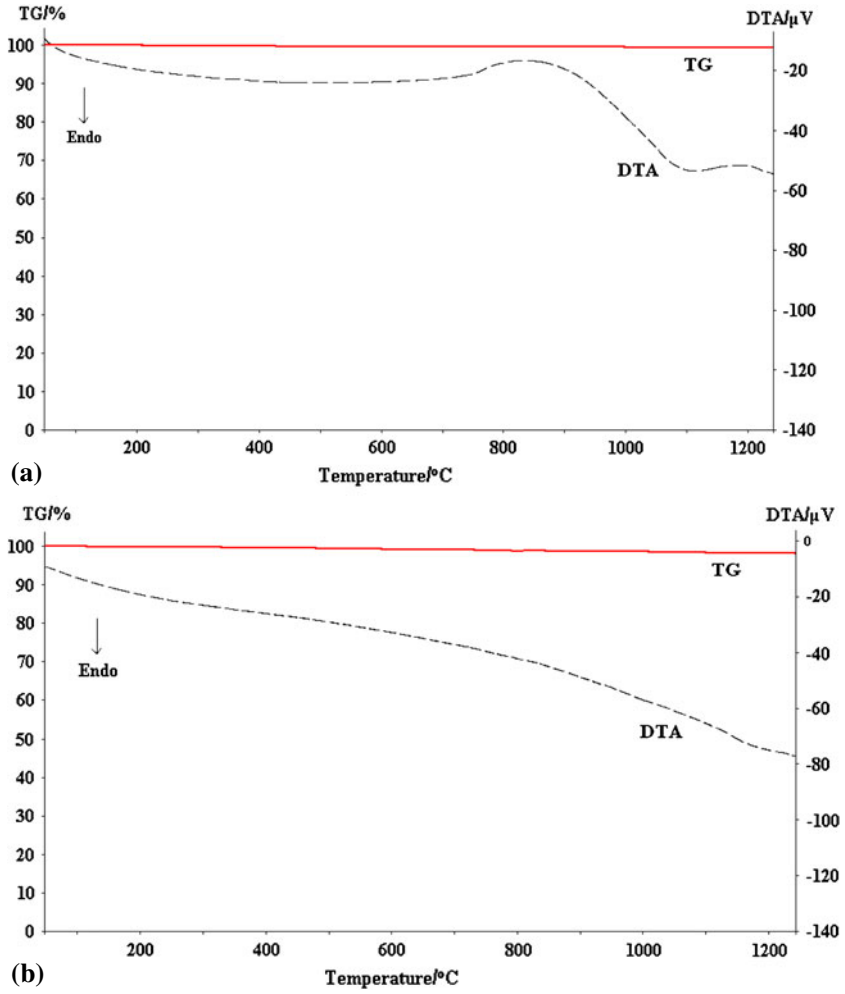

Figure 2. TG/DTA curves of (**a**) $MgTiO_3$ and (**b**) $SrTiO_3$ synthesized at 1000 °C.

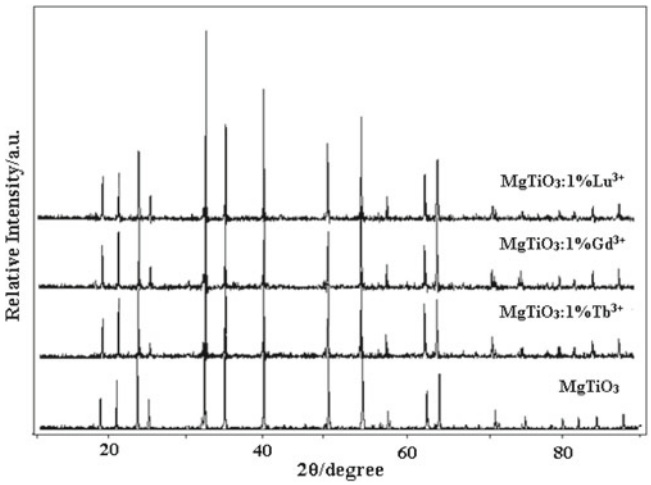

Figure 3. XRD patterns of $MgTiO_3$ and $MgTiO_3$:RE (RE = Gd^{3+}, Tb^{3+}, Lu^{3+}).

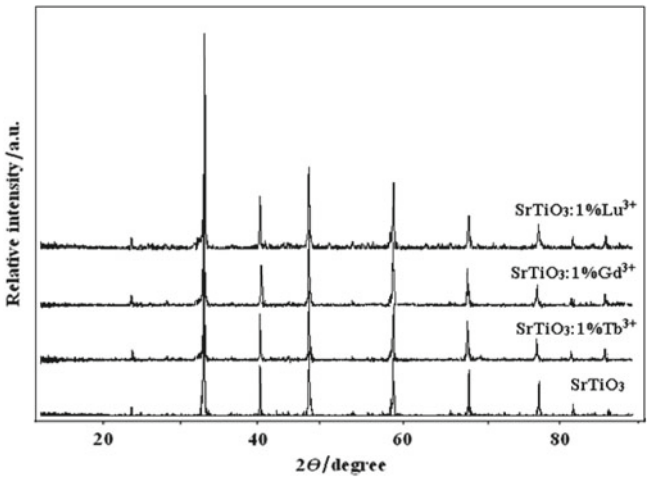

Figure 4. XRD patterns of $SrTiO_3$ and $SrTiO_3$:RE (RE = Gd^{3+}, Tb^{3+}, Lu^{3+}).

Table 1. Gd^{3+}, Tb^{3+} and Lu^{3+} in $MTiO_3$ (M = Mg and Sr) luminescence properties.

Samples	a (pm)	b (pm)	c (pm)	$V \times 10^6$ (pm^3)
$MgTiO_3$	505·40	505·40	1389·00	355
$MgTiO_3$:1 %Gd^{3+}	505·39	505·39	1390·49	355
$MgTiO_3$:1 %Tb^{3+}	505·40	505·40	1390·46	355
$MgTiO_3$:1 %Lu^{3+}	505·43	505·43	1390·46	355

Table 2. Unit cell parameters of $SrTiO_3$ and $SrTiO_3$:RE (RE = Gd^{3+}, Tb^{3+}, Lu^{3+}).

Samples	a (pm)	$V \times 10^5$ (pm^3)
$SrTiO_3$	390·50	596
$SrTiO_3$:1 %Gd^{3+}	390·51	596
$SrTiO_3$:1 %Tb^{3+}	390·51	596
$SrTiO_3$:1 %Lu^{3+}	390·52	596

Structural characterization was analysed by X-ray diffraction (XRD; Bruker AXS D8) spectra with a CuKα line of 1·5406 Å. Scanning electron microscopy (SEM) images and EDX analysis were taken with LEO 440 model scanning electron microscope using an accelerating voltage of 20 kV.

The excitation and emission spectra of phosphors were recorded by Perkin Elmer LS 45 model luminescence spectrophotometer with xenon lamp.

Thermoluminescence (TL) glow curves of phosphors were measured by using TL reader (Harshaw-QS 3500, Erlangen, Germany) at a linear heating rate of 1 °C/s up to 400 °C after irradiation using $^{90}Sr/^{90}Y$ β-source (2·2 MeV) at a dose rate of ∼0·04 Gy/s at *RT*.

3. Results and discussion

3.1 *Thermal behaviour, crystallization and morphology*

Thermal decomposition behaviours of the phosphors were examined by TG analysis under an inert N_2 atmosphere with a heating rate of 10 °C/min. We reported DTA/TG spectra of undoped $MgTiO_3$ in our previous study (Korkmaz and Kalaycioglu 2011). Figure 1 illustrates DTA/TG/DTG curves of nominal composition, $SrTiO_3$.

TG/DTG/DTA curves of the precursor are given in figure 1. Several obvious peaks are identified on DSC curve. Between 50 and 490 °C, the weight loss of 24% is due to the removal of butyl alcohol, indicated by two endothermic peaks on the DTA curve. From 520–610 °C, there is a weight loss of 23%, accompanied by the decomposition of $Sr(NO_3)_2$ which is transformed into SrO. Thus, $SrTiO_3$ powders may be formed in this temperature range.

TG/DTA curve patterns of $MgTiO_3$ and $SrTiO_3$ synthesized at 1000 °C are shown in figure 2. The samples did not loose mass and the phase change was not identified in temperatures between 48 and 1243 °C.

X-ray powder diffraction patterns for the undoped and 1 mol% RE-doped samples were identical. The diffraction patterns of all the samples matched with that of hexagonal $MgTiO_3$ with no impurity phase (JCPDS card files 6-494 (hexagonal; a = 505·40, c = 1389.80 (in pm)). One of the representative XRD patterns of $MgTiO_3$ and $MgTiO_3$:RE (RE = Gd^{3+}, Tb^{3+}, Lu^{3+}) calcined at 1000 °C is shown in figure 3. All the reflections observed in the patterns could be indexed to the respective planes for a system as given in table 1.

XRD patterns of $SrTiO_3$ and $SrTiO_3$:RE (RE = Gd^{3+}, Tb^{3+}, Lu^{3+}) calcined at 1000 °C are shown in figure 4. XRD patterns for these $SrTiO_3$:RE phosphors were measured and showed a similar crystalline system. XRD patterns were also found to be in good agreement with those of $SrTiO_3$ listed in JCPDS card files 35-0734 (cubic; a = 390·50 (in pm)). The unit cell parameters of the patterns in the crystallized system are listed in table 2.

Figures 5 and 6 show images and EDX analysis obtained from SEM of the phosphors calcined at 1000 °C for 2 h by using solid-state reactions. Microstructures of the phosphors consisted of regular fine grains with an average size of about 150–200 nm. EDX analysis of the chemical composition of the samples confirms results of the experimental evidence. EDX analysis results of the phosphors are listed in table 3.

3.2 *Photoluminescence and thermoluminescence properties*

Figure 7 shows excitation and emission spectra of the $SrTiO_3$, $SrTiO_3$:1 % Tb^{3+}, $SrTiO_3$:1 %Gd^{3+} and $SrTiO_3$:1 %Lu^{3+} phosphors annealed at 1000 °C. In the excitation spectra of the phosphors, a broad, excitation band is observed from 260–300 nm with a maximum at about 275 nm. The excitation and emission spectra of $MgTiO_3$, $MgTiO_3$:1 %Tb^{3+}, $MgTiO_3$:1 %Gd^{3+} and $MgTiO_3$:1 %Lu^{3+} are shown in figure 8. In the excitation spectra of the phosphors, a broad, excitation band is observed from 240 to 280 nm with a maximum at about 255 nm. Obviously, the excitation spectra of $MgTiO_3$ and $SrTiO_3$ bands are ascribed to a charge transfer (CT) from the oxygen ligands to the central titanium atom. The valence–conduction band transition Ti^{4+}–O^{2-} to Ti^{3+}–O^{-} is seen to occur (Ruza *et al* 1998). The addition of RE^{3+} atoms decreased the excitation intensity of the $SrTiO_3$ and $MgTiO_3$ phosphors (table 4).

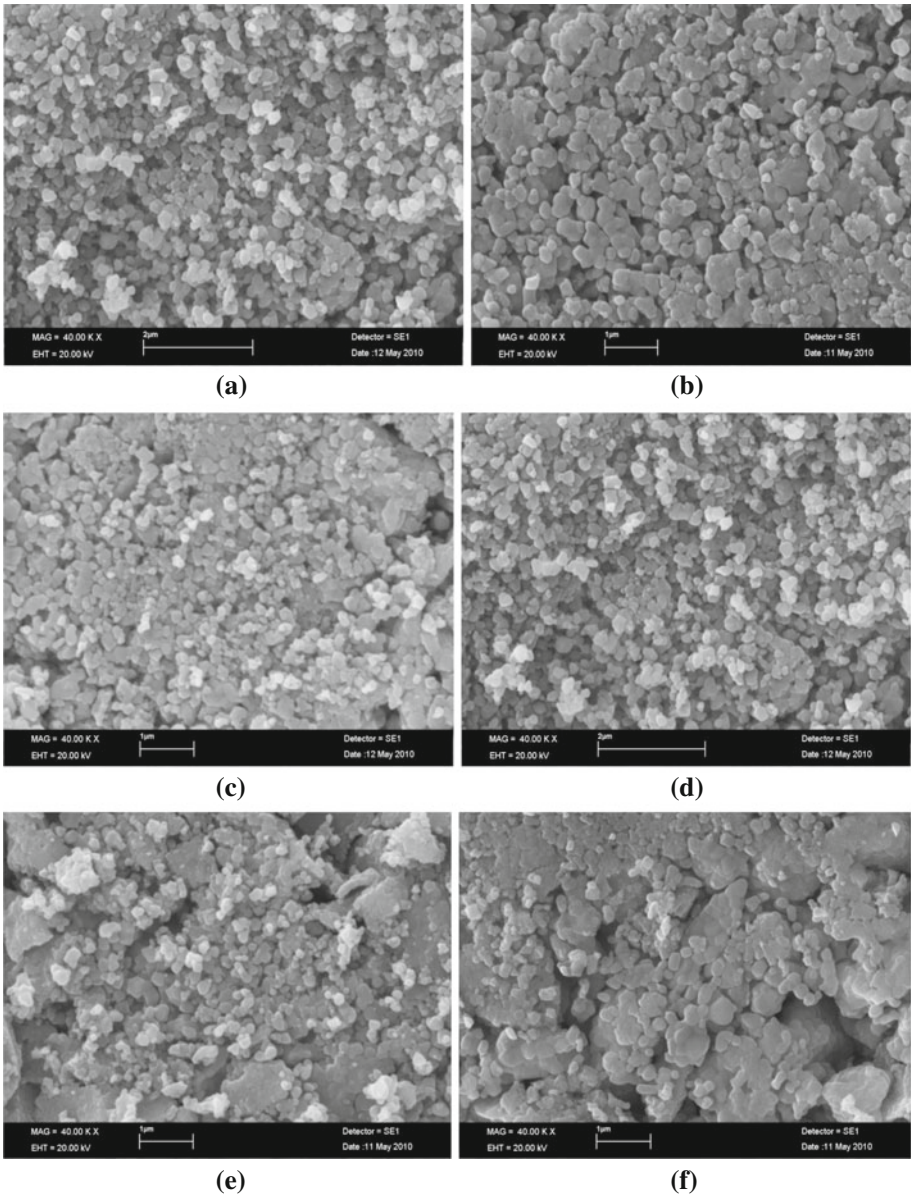

Figure 5. Representative SEM images of (**a**) $MgTiO_3$:1 %Tb^{3+}, (**b**) $MgTiO_3$:1 %Lu^{3+}, (**c**) $MgTiO_3$:1 %Gd^{3+}, (**d**) $SrTiO_3$:1 %Tb^{3+}, (**e**) $SrTiO_3$:1 %Lu^{3+} and (**f**) $SrTiO_3$:1 %Gd^{3+} phosphors.

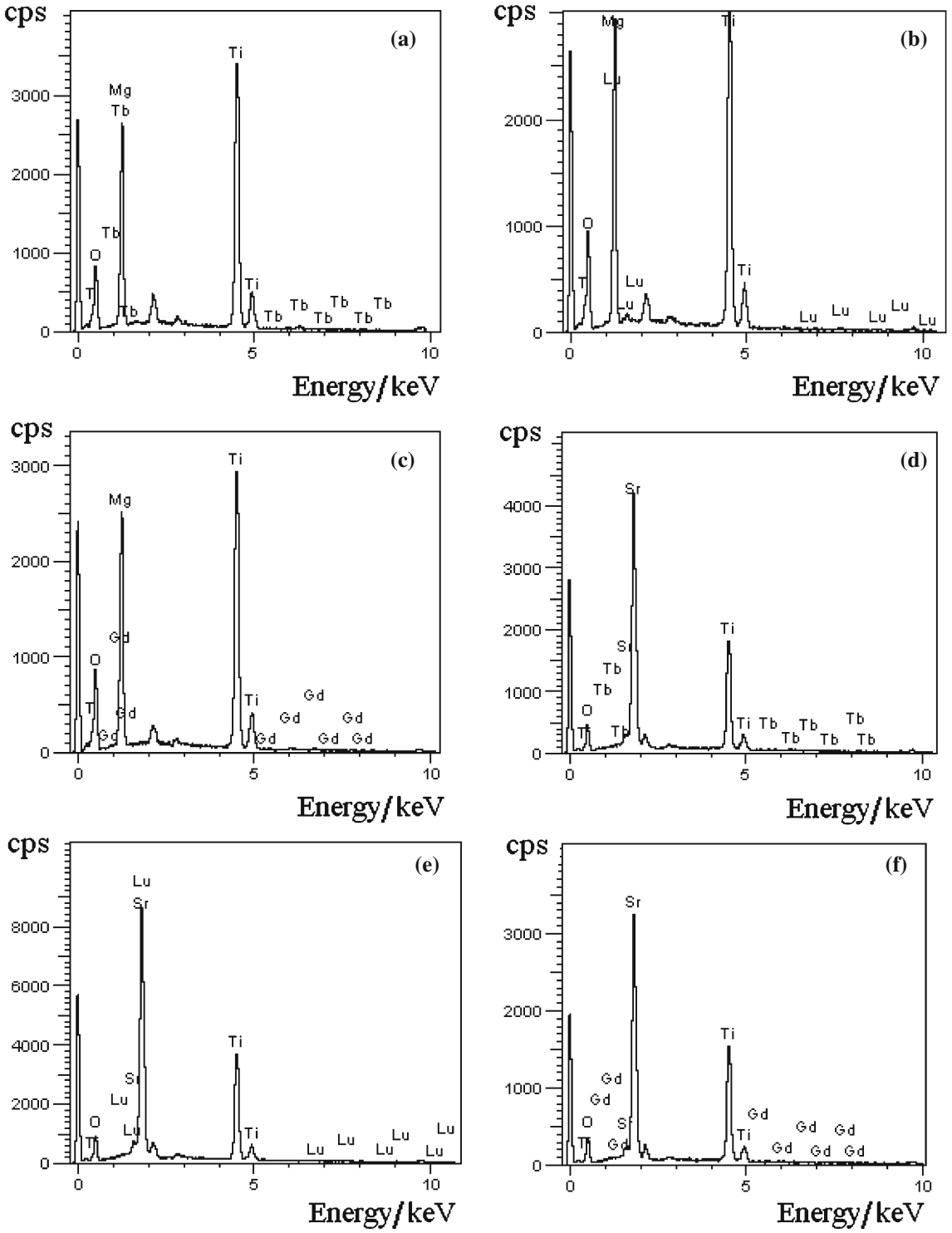

Figure 6. EDX analyses of (**a**) $MgTiO_3$:1 %Tb^{3+}, (**b**) $MgTiO_3$:1 %Lu^{3+}, (**c**) $MgTiO_3$:1 %Gd^{3+}, (**d**) $SrTiO_3$:1 %Tb^{3+}, (**e**) $SrTiO_3$:1 %Lu^{3+} and (**f**) $SrTiO_3$:1 %Gd^{3+} phosphors.

Characteristic transitions expected for the Tb^{3+} and Gd^{3+} ions were not observed. Typical emission peaks of Lu^{3+} were not observed in the emission spectra of $SrTiO_3$:1 %Lu^{3+} and $MgTiO_3$:1 %Lu^{3+} phosphors because, the Lu^{3+} ion has $4f^{14}5d^06s^0$ electronic configuration.

The doping of 1% mole Tb^{3+}, 1% mole Lu^{3+} and 1% mole Gd^{3+} ions to $MgTiO_3$ decreased radiation intensity by 185, 290 and 340 units, respectively. The doping of 1% mole Tb^{3+}, 1% mole Gd^{3+} and 1% mole Lu^{3+} ions to $SrTiO_3$ decreased radiation intensity by 145, 180 and 350 units, respectively.

Table 3. EDX analysis results of phosphors.

Phosphors	Theoretical				Experimental			
	M	Ti	O	RE^{3+}	M	Ti	O	RE^{3+}
$MgTiO_3$	20·22	39·84	39·94	–	19·65	38·13	42·22	–
$MgTiO_3$:1 %Gd^{3+}	19·96	39·32	39·43	1·29	18·84	38·13	41·73	1·30
$MgTiO_3$:1 %Tb^{3+}	19·95	39·32	39·43	1·30	18·07	40·77	39·80	1·36
$MgTiO_3$:1 %Lu^{3+}	19·93	39·27	39·37	1·43	19·55	37·44	41·51	1·50
$SrTiO_3$	47·75	26·09	26·16	–	49·85	24·24	25·91	–
$SrTiO_3$:1 %Gd^{3+}	47·35	25·87	25·93	0·85	49·04	25·59	24·48	0·89
$SrTiO_3$:1 %Tb^{3+}	47·35	25·87	25·92	0·86	48·54	24·73	25·78	0·95
$SrTiO_3$:1 %Lu^{3+}	47·30	25·85	25·91	0·94	49·39	24·78	25·01	0·82

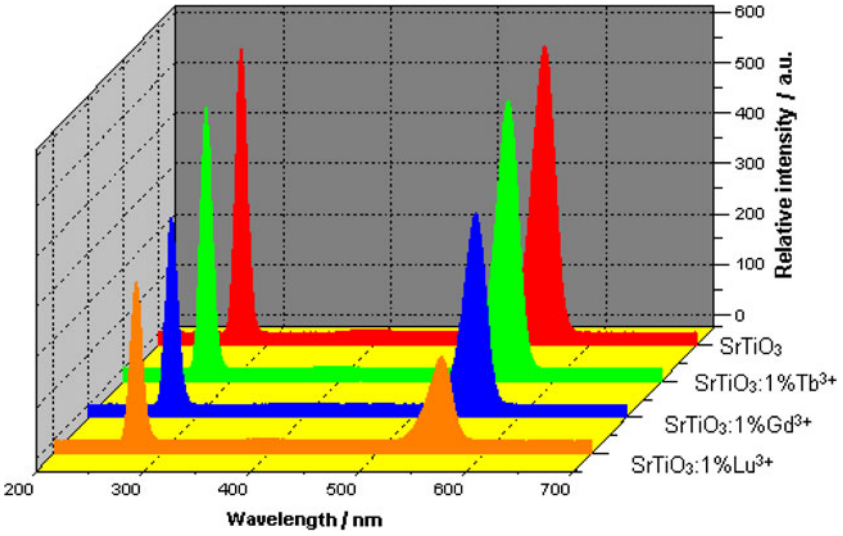

Figure 7. Excitation and emission spectra of $SrTiO_3$, $SrTiO_3$:1 %Tb^{3+}, $SrTiO_3$:1 %Gd^{3+} and $SrTiO_3$:1 %Lu^{3+}.

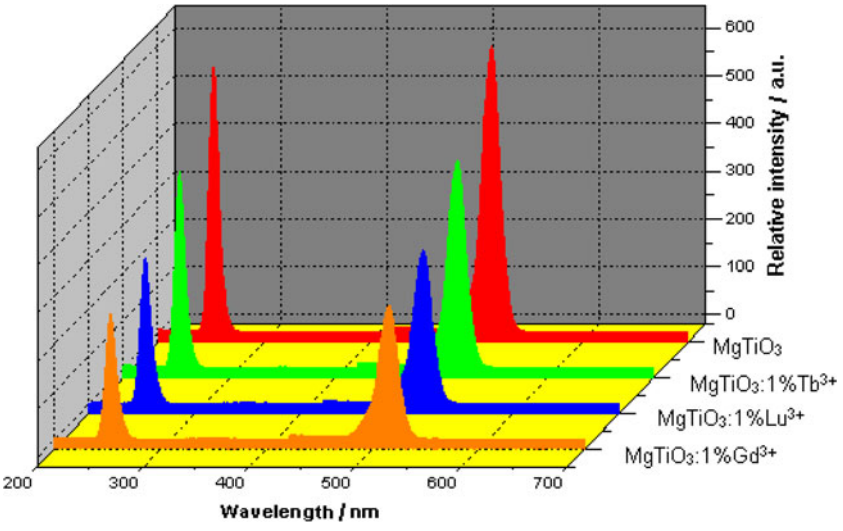

Figure 8. Excitation and emission spectra of $MgTiO_3$, $MgTiO_3$:1 %Tb^{3+}, $MgTiO_3$:1 %Gd^{3+} and $MgTiO_3$:1 %Lu^{3+}.

Table 4. Phosphorescence properties of phosphors.

Phosphors	Radiation intensity/a.u.	Radiation colour	Radiation wavelength (nm)	Undoped–doped radiation difference
$MgTiO_3$	600	Yellow	514	–
$MgTiO_3$:1 %Tb^{3+}	415	Yellow	514	−185
$MgTiO_3$:1 %Lu^{3+}	260	Yellow	514	−290
$MgTiO_3$:1 %Gd^{3+}	310	Yellow	514	−340
$SrTiO_3$	660	Yellow	559	–
$SrTiO_3$:1 %Tb^{3+}	515	Yellow	558	−145
$SrTiO_3$:1 %Gd^{3+}	480	Yellow	560	−180
$SrTiO_3$:1 %Lu^{3+}	310	Yellow	558	−350

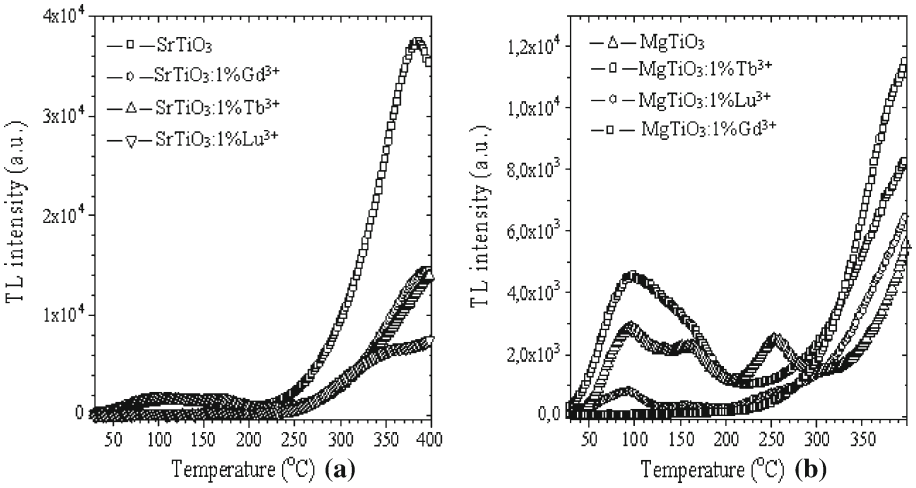

Figure 9. TL glow curves of (**a**) $SrTiO_3$ and $SrTiO_3$:RE (RE = Gd^{3+}, Tb^{3+}, Lu^{3+}) and (**b**) $MgTiO_3$ and $MgTiO_3$:RE (RE = Gd^{3+}, Tb^{3+}, Lu^{3+}) phosphors ($D \approx 36$ Gy and $\beta = 1$ °C s^{-1}).

The change in the radiation intensities of the doped ions can be attributed to two different reasons. The first reason is that defect centres occurring in the host crystal due to the doping of ions can increase radiation intensity. The second is that trap centres emerging with doping can decrease the radiation intensity by acting as an extinction centre.

Thermoluminescence (TL) properties of $MgTiO_3$ and $SrTiO_3$ samples doped with Gd^{3+}, Tb^{3+} and Lu^{3+} were also investigated. The samples were irradiated at room temperature with a newly calibrated ^{90}Sr–^{90}Y beta source ($D \approx 0{\cdot}04$ Gy/s). Glow curve readout was carried out on a platinum planchet at a linear heating rate of 1 °C/s up to 400 °C. As seen from figure 9, phosphors do not show TL characteristic.

4. Conclusions

In conclusion, yellow phosphors doping with Gd^{3+}, Tb^{3+} and Lu^{3+} in $MTiO_3$ (M = Mg and Sr) were synthesized by a modified solid-state reaction at 1000 °C. $MgTiO_3$ and $MgTiO_3$:RE (RE = Gd^{3+}, Tb^{3+}, Lu^{3+}) and $SrTiO_3$ and $SrTiO_3$:RE (RE = Gd^{3+}, Tb^{3+}, Lu^{3+}) phosphors were shown to have a hexagonal and cubic structure, respectively. The average diameters of the grain size of the materials were in the range of 150–200 nm. The addition of RE^{3+} atoms decreased the excitation intensity of the $SrTiO_3$ and $MgTiO_3$ phosphors and phosphors do not show TL characteristic.

Acknowledgement

This work was financially supported by Erciyes University's Research Fund (BAP-FBY 09-861 2009).

References

Blasse G 1989 *Chem. Mater.* **1** 294
Cavalli E, Speghini A, Bettinelli M, Ramirez M O, Romero J J and Bausa L E 2003 *J. Lumin.* **216** 216
Doat A, Pelle F and Lebugle A 2005 *J. Solid State Chem.* **178** 2354
Freitas G F G, Nasar R S, Cerqueira M, Melo D M A, Longo E and Varel J A 2006 *Mater. Sci. Eng.* **A434** 19
Hu L, Song H, Pan G, Yan B, Qin R and Dai Q 2007 *J. Lumin.* **127** 371
Jia C W, Xie E Q, Zhao J G, Sun Z W and Peng A H 2006 *J. Appl. Phys.* **100** 23529

Korkmaz E and Ozpozan Kalaycioglu N 2011 *J. Therm. Anal. Calorim.*; doi: 10.1007/s10973-011-2139-8

Lima R C *et al* 2006 *J. Appl. Phys.* **100** 34917

Lina K M, Lina C C, Hsiaob C Y and Lia Y Y 2007 *J. Lumin.* **127** 561

Moreira M L, Gurgel M F C, Mambrini G P, Leite E R, Pizani P S and Varela J A 2008 *J. Phys. Chem.* **A112** 8938

Naik Y P, Mohapatra M, Dahale N D, Seshagiri T K, Natarajan V and Godbole S V 2009 *J. Lumin.* **129** 1225

Park J K, Lim Mi A, Kim C H, Park H D, Park J T and Choi Se Y 2003 *Appl. Phys. Lett.* **82** 683

Park J K, Ryu H, Park H D and Choi S Y 2001 *J. Eur. Ceram. Soc.* **21** 535

Ruza E, Reyher H J and Trokss J, Wöhlecke M 1998 *J. Phys.: Condens. Matter.*; doi: 10.1088/0953-8984/10/19/017

Singh V, Zhu J J, Tiwari M, Soni M, Aynayas M and Hyun S H 2009 *J. Non-Cryst. Solids* **355** 2491

Sinha A, Nair S R and Sinha P K 2010 *J. Nucl. Mater.* **399** 162

Wickersheim K A and Lefever R A 1964 *J. Electrochem. Soc.* **111** 47

Wuled Lenggoro I, Panatarani C and Okuyama K 2004 *Mater. Sci. Eng.* **B113** 60